Available online at www.sciencedirect.com
SCIENCE DIRECT®
Journal of Solid State Chemistry 177 (2004) 1508–1512
JOURNAL OF SOLID STATE CHEMISTRY
http://elsevier.com/locate/jssc

Dielectric characteristics of a Ce^{3+}-doped $Sr_{0.61}Ba_{0.39}Nb_2O_6$ single crystal with Cole–Cole plots technique

E. Şentürk[a,b,*]

[a] Department of Physics, Gebze Institute of Technology, Gebze, Kocaeli 41400, Turkey
[b] Department of Physics, Sakarya University, Sakarya, Sakarya 54100, Turkey

Received 15 August 2003; received in revised form 18 November 2003; accepted 2 December 2003

Abstract

In this paper, we have investigated relaxation mechanisms and dielectric characteristics of an $Sr_{0.61-x}Ba_{0.39}Nb_2O_6Ce_x$ (abbreviated as SBN61 and $x = 0.0066$) single crystal with dielectric spectroscopy measurements. The crystal undergoes a ferroelectric phase transition at 340 K. The temperature dependence of the real and imaginary part of the complex dielectric susceptibility in the vicinity of ferroelectric–paraelectric phase transition has been studied in the frequency region 100 Hz–10 mHz. The measurement of the dielectric constants of the real and imaginary parts shows strong frequency dependence. The investigations of the dielectric constant using Cole–Cole plots revealed a non-Debye-type dielectric relaxation for Ce^{+3}-doped SBN61. It reveals the coexistence of the two dielectric relaxators in the vicinity of the phase transition.

Keywords: Cole–Cole plots; Dielectric relaxation; Ferroelectrics

1. Introduction

The dielectric behavior of materials under external AC field has been the focus of numerous papers, in view of its high scientific and technological importance. The measurements are made in wide frequency and temperature ranges for many types of materials [1].

Strontium–barium niobate ($Sr_xBa_{1-x}Nb_2O_6$) is a promising material due to its very attractive piezoelectric [2], electrooptic [3,4], acoustooptic [5], photorefractive [6,7] and nonlinear optic [8] properties.

$Sr_{0.61}Ba_{0.39}Nb_2O_6$ belongs to the tetragonal tungsten bronze ferroelectric oxide family of the general formula AB_2O_6 [9]. The congruently melting SBN61 composition is a bronze with small unit cell. The high-temperature prototype symmetry is tetragonal $4/mm$ as determined by X-ray diffraction investigation [10]. This double solid solution system may be represented by the structural formula $A'_2A''_4C_4B'_2B''_8O_{30}$ which takes into account the total number of different sites and non-equivalency of the oxygen octahedral. The twelve-fold (A') coordinated sites are occupied only by smaller Sr^{2+} ions, the fifteen-fold (A'')—both by the Sr^{2+} and Ba^{2+} ions, whereas the smallest nine-fold coordinated vacancies are empty. Since only 5/6 of the A sites are occupied, SBN61 is referred to as an unfilled bronze and the vacancies of the other 1/6 A sites act as carrier trapping centers [11]. A ferroelectric unit cell contains five formal AB_2O_6 and five formal AB_2O_6. The high-temperature prototype symmetry is tetragonal $4/mm$ [9].

Doping with Ce^{3+}, where only the Sr^{2+} sites are occupied [9], strongly lowers the phase transition temperature, T_c [9]. Ce^{3+}-doped $Sr_{0.61}Ba_{0.39}Nb_2O_6$ undergoes a ferroelectric phase transition at $\sim$340 K.

In contrast with the pure SNB61 system, the doped ones are of practical importance. It is well-known that dopants enhance various physical properties. In particular, SBN61 doped with rare-earth metal ions are most efficient photorefractive materials widely used for holographic applications [12].

Relaxator ferroelectrics are characterized by a broad maximum in the temperature dependence of the dielectric permittivity and significant frequency dependence of their peak permittivity, persistence of the local polarization far above the phase transition temperature T_c, absence of macroscopic spontaneous polarization

*Corresponding author. Department of Physics, Gebze Institute of Technology, Gebze, Kocaeli 41400, Turkey. Fax: +90-262-6538490.
E-mail address: esenturk@gyte.edu.tr.

0022-4596/$ - see front matter © 2003 Elsevier Inc. All rights reserved.
doi:10.1016/j.jssc.2003.12.001

and structural symmetry breaking after zero-field cooling.

The measurements reveal that there are two relaxation mechanisms in Ce^{+3}-doped SBN61 while there is a single relaxator in undoped SBN61. In the literature there is no evidence that Ce^{+3}-doped SBN61 has two relaxators in the vicinity of the phase transition temperature. The aim of this paper is to clarify the nature of the relaxation mechanisms with Cole–Cole plots technique and reveal dielectric parameters by fitting non-Debye-type formula.

2. Experimental details

Ce^{+3}-doped SBN61 crystals were grown by the Czochralski technique. The samples, which were in rectangular form, were oriented along the polar axis which lies in the cleavage plane (the morphology of crystals permits cleavage to plane parallel plates with mirror-like surfaces). The plates were gently polished and cleaned. The crystal surface was covered with pure copper by using an evaporating system. In order to prevent oxidation of the electrodes the copper was covered with a silver paste. Samples shaped as bars for dielectric measurements were plates of dimensions of about $5 \times 4\,mm^2$ with an inter-electrode distance of 1 mm.

The capacitance bridge method, which has advantages such as high accuracy and wide frequency coverage, was used. The measurements of the complex dielectric permittivity, $\varepsilon^* = \varepsilon' - i\varepsilon''$, were carried out with 4194A model HP Impedance/Gain-Phase Analyzer as a function of temperature (320–400 K) and frequency (100 Hz–10 mHz) in a DC electric field. The instrument sensitivity is about 0.001 fF. The system is fully computer controlled with software written in Visual Borland Delphi program. The heating rate was maintained at 1 K/min and the data were recorded in a personal computer under isothermal conditions. The sensitivity of Lakeshore 340 model temperature controller was about 0.001 K.

The dielectric constants were measured in a temperature range between 320 and 400 K. For each temperature, at least 30 (for 380 K) frequencies were applied.

3. Results and discussion

Fig. 1a shows the temperature dependence of the real and imaginary part of the dielectric constant of the sample in the frequency range from 100 Hz–10 mHz. It is observed from the figure that the peaks of the dielectric spectra show strong temperature and frequency dependence. The peaks are significantly shifted towards higher temperatures. The magnitude of the real part of the dielectric constant strongly drops at high frequencies. The peaks clearly become broader. They are flattened and weakly temperature dependent at 10 mHz. The real part of the dielectric constant is independent of temperature at frequencies higher than 10 mHz.

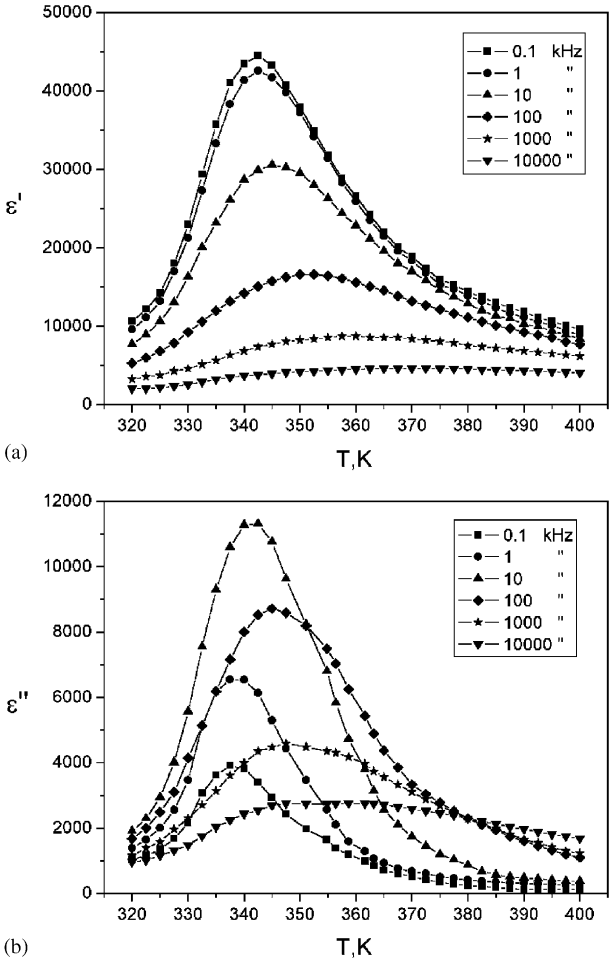

Fig. 1. The temperature dependence of (a) the real part, (b) the imaginary part of the dielectric constant at various frequencies.

The imaginary part of the dielectric constant at some fixed frequencies has been plotted as a function of temperature in Fig. 1b. It is evident from the figure that the peaks shift to higher temperatures with increasing frequency. Moreover, the magnitude of the peak first increases and then, decreases with increasing frequency. This is clearly an evidence for the polydispersive-type relaxation mechanism in Ce^{3+}-doped SBN61.

Dielectric relaxation experiments at various frequencies have given us some information such as relaxation times, possible relaxators and their activation energies. The Cole–Cole plots are a good technique in order to investigate relaxation mechanisms in ferroelectric materials. Well-defined portions of circles overlapping each other and passing through the ε' axis near the origin were obtained in the vicinity of the phase transition temperature. Two relaxations are clearly observed in the

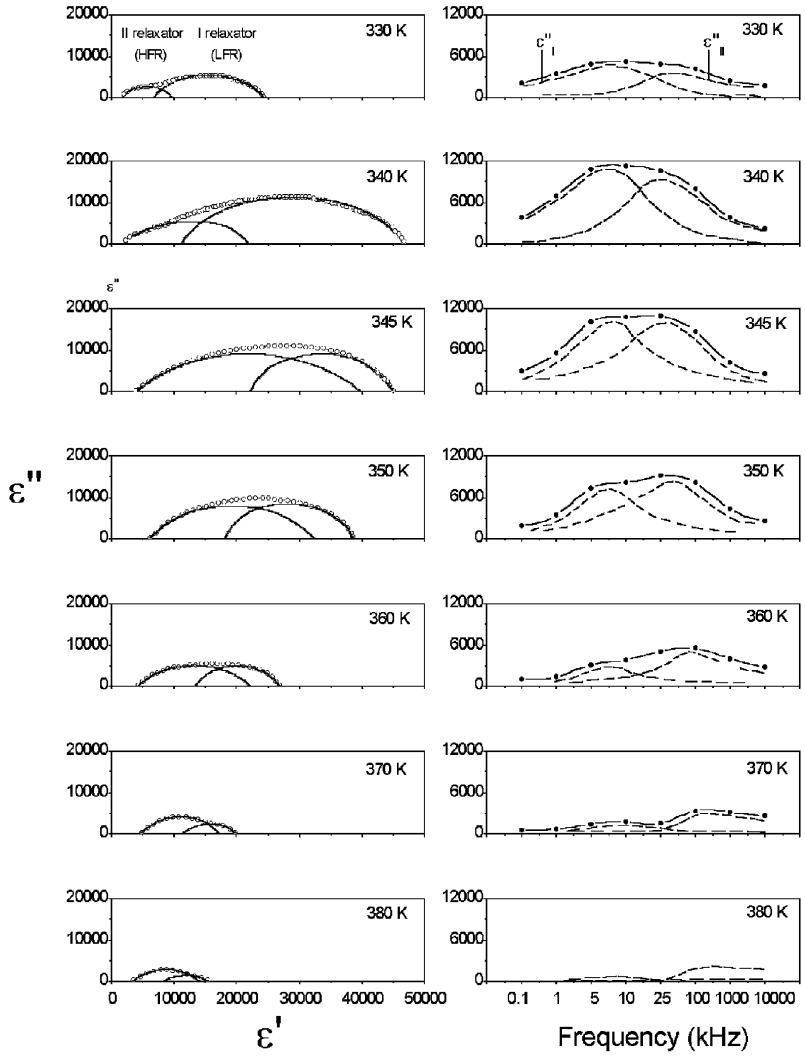

Fig. 2. The variation of imaginary part with real part of dielectric constant at various temperatures (left side) and the imaginary part of dielectric constant with frequency (right side), respectively.

dielectric spectrum of the imaginary part and semicircles shown in Fig. 2. The presence of two semicircles in the complex plane permittivity indicates the polydispersive nature of the dielectric properties of the crystal. In the description of dielectric relaxations, a generalized Debye model gives the Cole–Cole representation of the frequency-dependent complex permittivity ε^* presented by the well-known expression [13].

$$\varepsilon^*(w) = \varepsilon'(w) - \varepsilon''(w) = \varepsilon_\infty + \frac{\varepsilon_{s1} - \varepsilon_{s2}}{1 + (iw\tau_1)^{1-\alpha_1}} + \frac{\varepsilon_{s2} - \varepsilon_\infty}{1 + (iw\tau_2)^{1-\alpha_2}}.$$

Here, w denotes the measuring frequency, τ_1 and τ_2 are the relaxation times of relaxators I and II, α_1 and α_2 are the angles of the semicircular arcs shown in Fig. 3 ($1 \geqslant \alpha \geqslant 0$). The parameter, α, represents a measure of the width of the distribution of the relaxation time. The

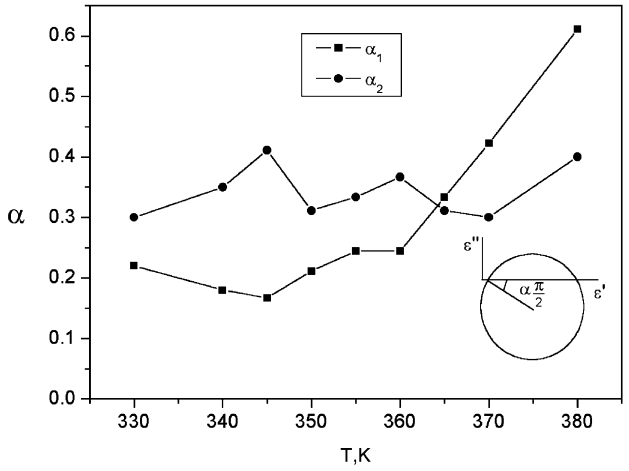

Fig. 3. The variation of the widths of the distributions of relaxation times with temperature.

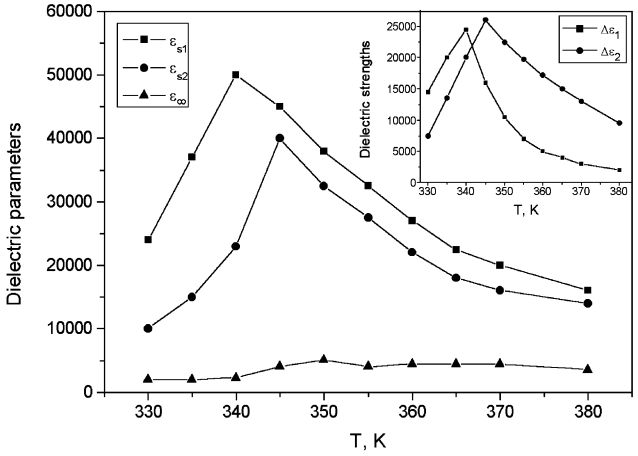

Fig. 4. The dielectric characteristics versus temperature.

values of α are estimated from Cole–Cole plots by measuring the angle between the ε' axis and radius of the circle (inset of the Fig. 3). If the centers of the semicircles lie on the ε' axis, α is zero (Debye type), otherwise the center is below the ε' axis and $\alpha \neq 0$ (non-Debye type). ε_{s1} and ε_{s2} are the limiting values of permittivity of the relaxators (I and II). ε_∞ is the high-frequency limit of the dielectric constant. The parameters, $\Delta\varepsilon_1 = \varepsilon_{s1} - \varepsilon_{s2}$ and $\Delta\varepsilon_2 = \varepsilon_{s2} - \varepsilon_\infty$, are known as the dielectric strengths of these relaxations. The relaxation strengths of $\Delta\varepsilon_1$ and $\Delta\varepsilon_2$ can be obtained from extrapolation of arcs in Fig. 2. The results are shown in (inset) Fig. 4. The dispersion strengths exhibit two different maxima. As can be seen from this figure, the dielectric strengths of $\Delta\varepsilon_1$ and $\Delta\varepsilon_2$ relaxators rise below the phase transition temperature and then, diminish above the phase transition temperature. However, the dielectric strength of the second relaxator diminishes monotonically and the dielectric strength of first relaxator diminishes more quickly than the first one in paraphase.

From the Cole–Cole plots (Fig. 2) a coexistence of the two contributions is observed in the paraelectric-ferroelectric phase. The low-frequency relaxator (LFR or relaxator I) exists in the frequency range of 0.1–25 kHz and the high-frequency relaxator (HFR or relaxator II) contributes in the range of 25 kHz–10 mHz. The relaxation type of the crystal is non-Debye type because $\alpha \neq 0$. The width of the distribution of the relaxation times (α_1,α_2) and dielectric characteristics (ε_{s1}, ε_{s2} and ε_∞) are given in Figs. 3 and 4, respectively. The relaxators have different temperature dependence of their relaxation frequencies. The high- and low-frequency relaxators have increasing amplitude until phase transition temperature and then, decreasing amplitude with increasing temperature (right side in Fig. 2). The amplitude of relaxator I increases faster than that of relaxator II. It can be concluded from this that the main contribution to the imaginary part of the dielectric constant comes from low-frequency relaxator (I) in the ferroelectric phase. The amplitude of relaxator I decreases faster than that of the relaxator II and vanishes at temperatures above 380 K. It is concluded from this that the main contribution to the imaginary part of the dielectric constant comes from high-frequency relaxator (II) in the paraelectric phase. In addition, it is a general reality that the low frequencies (relaxator I) are the main contributors for the real part of the dielectric constant in the full range of temperature.

The data could be well fitted by two non-Debye-type relaxations. In relaxation equation, all invariable parameters have been determined from the Cole–Cole plots except τ_1 and τ_2. It has been written on a simple Fortran program for fitting process. It has two different variables (τ_1 and τ_2) and four invariables (ε_{s1}, ε_{s2}, ε_∞ and w). The program comprises two main vicious circles associated with the relaxation times. The fitting parameters have been calculated by selecting two proper starting values for relaxation times at a fixed temperature and frequency. The same process has been carried out for all frequencies at the same fixed temperature and an average value has been taken separately for τ_1 and τ_2. All fitting procedures were carried out for all temperatures. Fig. 5 shows the calculated results of relaxation times for each relaxator. When the temperature increases, the relaxation time for each relaxator becomes longer in the ferroelectric phase and shorter in the paraelectric phase. As can be seen from Fig. 5, the main feature is that the two relaxation time curves intersect in the temperature range of 365–370 K. After this, the first relaxator relaxes more quickly than the second one and before that vice versa.

The temperature dependence of the relaxation time provides some insights into the structure of the crystal. The kinetics of the dielectric relaxation largely depends upon the characteristics of the relaxation site. Namely, the crystal may also have two kinds of relaxation sites

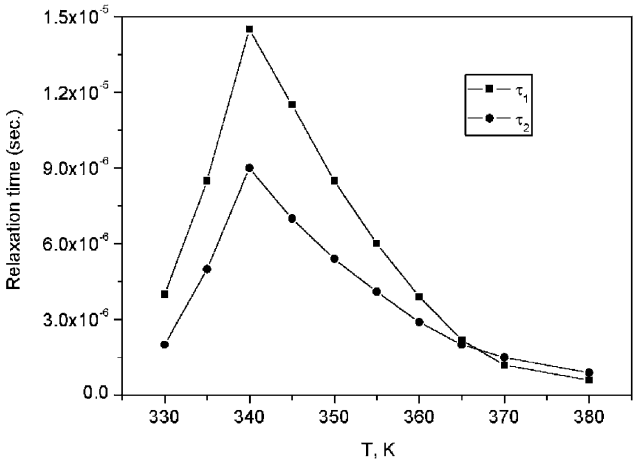

Fig. 5. Relaxation times versus temperature.

associated with two different characteristic relaxation times. The rapid decay of the relaxation time of the sample in the paraelectric phase is associated with shrinking of domains leading to an increased density of domain walls and vice versa in the ferroelectric phase.

In this study, specimens prepared from a high-quality single crystal were used. The samples were gently polished and then purified three times. The specimen thickness was 1 mm and a weak electric field was adopted, which is lower than the limit of the linear dielectric behavior. This induces us to consider the results obtained in this study as highly credible. If the dielectric data are compared with [14], it can be realized that the crystal quality is high. The characteristic dielectric relaxation time is directly related to the quality and sample preparation conditions. A plausible explanation for the relatively high dielectric relaxation time can be given by considering the crystal quality. Namely, the high-quality crystal has less defects and imperfections, as a result of this, the characteristic relaxation time is prolonged.

4. Conclusions

The dielectric spectroscopy is a powerful technique for characterizing the influence of dopants in dielectrics. The Cole–Cole plots reveal that there are two relaxation mechanisms in Ce^{+3}-doped SBN61 while there is a single relaxator in undoped SBN61.

The crystal has a strange relaxation mechanism. The dielectric relaxation of materials can be developed due to substitution at low content of Ce^{3+} ions [13]. The relaxators gain power with $=$increasing temperature in the ferroelectric phase and lose their power with increasing temperature in paraphase. The high-frequency relaxator (II) is responsible for the main contribution to the imaginary part of the dielectric constant in the paraelectric phase. However, the low-frequency relaxator (I) is responsible for the main contribution at temperatures lower than phase transition (ferroelectric phase). In addition, the crystal has a very low dielectric relaxation time ($\sim 10^{-6}$ s).

References

[1] P.Q. Mantas, J. Eur. Cer. Soc. 19 (1999) 2079–2086.
[2] R.R. Neurgoankar, M.H. Kalisher, T.C. Lim, E.J. Staples, K.L. Keester, Mater. Res. Bull. 15 (1980) 1235.
[3] K. Tada, T. Murai, M. Aoki, K. Muto, K. Awazu, Jpn. J. Appl. Phys. 11 (1972) 1622.
[4] R.R. Neurgoankar, W.K. Cory, J.R. Oliver, Ferroelectrics 51 (1972) 3.
[5] E.L. Venturini, E.G. Spencer, A.A. Ballman, J. Appl. Phys. 40 (1969) 1622.
[6] B. Fisher, M. Cronin-Golomb, J.O. White, A. Yariv, R.R. Neurgoankar, Appl. Phys. Lett. 40 (1982) 863.
[7] R.R. Neurgoankar, W.K. Cory, J.R. Oliver, M.D. Ewbank, W.F. Hall, Opt. Eng. 26 (1987) 392.
[8] S.C. Abrahams, P.B. Jamieson, J.L. Bernstein, J. Chem. Phys. 54 (1971) 2355.
[9] J. Dec, W. Kleemann, Th. Woike, R. Pankrath, Eur. Phys. J. B 14 (2000) 627.
[10] J.R. Oliver, R.R. Neurgoankar, L.E. Cross, J. Appl. Phys. 64 (1988) 37.
[11] L.A. Shuvalov, J. Phys. Soc. Japan 28 (1970) 38.
[12] Th. Woike, T. Volk, U. Dörfler, R. Pankrath, L. Ivleva, M. Wöhlecke, Ferroelectr. Lett. 23 (1998) 127.
[13] Cz. Pawlaczyk, R. Jakubas, Solid State Commun. 113 (2000) 251–255.
[14] W. Kleemann, J. Dec, P. Lehnen, R. Blinc, B. Zalar, R. Pankrath, Eur. Lett. 57 (1) (2002) 14–19.